

## Error estimation and empirical geothermobarometry for pelitic systems

K. V. HODGES AND P. D. CROWLEY

Department of Earth, Atmospheric and Planetary Sciences  
Massachusetts Institute of Technology, Cambridge, Massachusetts 02139

### Abstract

Empirical calibration of net-transfer and exchange equilibria as geologic thermobarometers involves the use of input parameters, such as independent estimates of pressure and temperature, which can have large uncertainties. We present a calibration method which propagates these uncertainties into uncertainties in reaction enthalpy and entropy. The uncertainties calculated using this method are only semi-quantitative, because the correlation between errors in the various input parameters is virtually impossible to quantify. Nevertheless, the results offer a means of testing the relative precision of various empirical and experimental thermobarometers.

Using this technique, we present empirical calibrations for ten fluid-independent, net-transfer reactions in the pelitic system (KCFASH). The calibrations are based on pressure and temperature estimates derived using the garnet–biotite geothermometer and the garnet–plagioclase–aluminum silicate–quartz geobarometer. Some of the calibrations are excellent, and could lead to important new  $P$ – $T$  constraints for samples which do not contain biotite or aluminum silicate. However, propagation of uncertainties in  $\Delta H$ ,  $\Delta S$  and microprobe data into uncertainties in  $P$ – $T$  estimates suggests that even the best calibrated empirical thermobarometers are much less precise than the experimental thermobarometers on which they are based.

### Introduction

Empirical calibrations of exchange and net-transfer equilibria for geologic thermobarometry (e.g., Thompson, 1976a; Ghent and Stout, 1981) are becoming increasingly popular with metamorphic petrologists because empirical calibration is much simpler than its experimental counterpart, and because the results may be more readily applicable to complex natural systems. Little has been written, however, about the precision of  $P$ – $T$  estimates derived from empirical calibrations, and how this precision compares with that of thermobarometry based on experimental calibrations. In this study, we develop a scheme by which the uncertainties involved in empirical calibration may be propagated through both the calibration process and subsequent application of an equilibrium as a geothermometer or geobarometer. The technique is based on a linear regression method commonly used in geochronologic studies (York, 1969). This method, unlike many simpler linear regression routines, allows the incorporation of errors in  $x$  and  $y$  and their propagation into the calculated slope and  $y$ -intercept. We use our technique to calibrate 10 fluid-independent equilibria in the common pelitic assemblage: garnet–biotite–muscovite–plagioclase–aluminum silicate–quartz. Finally, we evaluate the precision with which temperatures and pressures can be calculated for natural samples using these thermobarometers.

### Technique

For any fluid-independent reaction, the equilibrium condition at  $P$  and  $T$  of interest may be written

$$0 = \Delta H - T\Delta S + (P - 1)\Delta V + RT \ln K, \quad (1)$$

where  $\Delta H$ ,  $\Delta S$ , and  $\Delta V$  are the enthalpy, entropy and volume of reaction, respectively. The equilibrium constant ( $K$ ) for this reaction is a function of mineral composition and (if the mineral solutions are non-ideal)  $P$  and  $T$ .

Empirical calibration of this reaction as a thermobarometer involves: (a) selection of a suite of  $n$  naturally occurring samples for which  $P$  and  $T$  can be estimated using previously calibrated equilibria; (b) calculation of  $P$ ,  $T$  and  $K$  for each sample using microprobe data and solution models; (c) estimation of  $\Delta V$ , the best known thermodynamic constant, using tabulated thermochemical data; and (d) simultaneous solution of  $n$  equations such as equation (1) for  $\Delta H$  and  $\Delta S$ . If more than two samples are used in this process, the thermodynamic unknowns are over-constrained by the resulting system of equations. Such multiplicity can be used to provide an estimate of the uncertainties in  $\Delta H$  and  $\Delta S$ , which are a consequence of the assumptions and the uncertainties in the empirical technique. One method of solving the necessary equations involves: (a) rewriting equation (1) as

$$(P - 1)\Delta V + RT \ln K = -\Delta H + T\Delta S; \quad (2)$$

b) plotting the calibration data as  $[x] = T$  vs.  $[y] = (P - 1)\Delta V + RT \ln K$ ; and c) using some form of least-squares linear regression analysis to calculate a slope ( $\Delta S$ ) and a  $[y]$ -intercept ( $-\Delta H$ ) for the resulting "linear" array.

The choice of regression treatment for this exercise is far from straightforward. It is tempting to dismiss uncertainties in  $[x]$  and  $[y]$  as small in comparison to the scatter of data about the best-fit line, and use one of many available regression treatments which assume no uncertainty in  $[x]$  or  $[y]$  and yield regression statistics which only reflect scatter in the data. However, the uncertainties in  $\Delta H$  and  $\Delta S$  obtained in this fashion can be misleading when the uncertainties in  $[y]$  and  $[x]$  are large, as they are likely to be when dealing with empirical data.

Regression situations in which the uncertainties in individual points are large in comparison to the scatter of the points about a best-fit line are common in geochronology, and a variety of regression treatments have been developed specifically for such applications (see Brooks et al., 1972, for a review). We will adopt the treatment developed by York (1969) which provides for correlated uncertainties in  $[y]$  and  $[x]$  and yields estimates of errors in slope and  $[y]$ -intercept that are dependent primarily on uncertainties in  $[y]$  and  $[x]$ . In principle, this treatment will yield realistic regression statistics whenever uncertainties in  $[x]$  and  $[y]$  are significantly greater than the data scatter.

For the empirical calibration situation, uncertainties in  $[x]$  are simply the uncertainties in estimated equilibration temperatures for the samples used. Uncertainties in  $[y]$  include: a) uncertainties in  $P$  and  $T$  as estimated by independent thermobarometry; b) uncertainties in  $\Delta V$  as calculated from thermochemical data; c) uncertainties in the microprobe analyses used to calculate mole fractions of phase components; and d) uncertainties in the activity models used to derive  $K$  from the appropriate phase components. We have a choice of two basic methods by which these uncertainties may be propagated into  $\sigma_{[y]}$ : the standard error propagation equation and the Monte Carlo method (Anderson 1976, 1977). The first method is the most rigorous in that it allows for covariance between parameters, but it is computationally difficult. The second approach is much simpler, but it does not account for covariance. In the case of  $[y]$ , some of the input parameters have highly correlated uncertainties (e.g.,  $P$  and  $T$ ), whereas others have essentially independent uncertainties (e.g., the microprobe data). Thus, we can partition  $[y]$  into terms for which  $\sigma$  can be reasonably estimated, using the simpler Monte Carlo method, and terms for which  $\sigma$  must be determined, using the rigorous error propagation equation.

We have assumed that the uncertainties incorporated onto  $\sigma_K$  are virtually uncorrelated or, at worst, that the covariances involved have little effect on the magnitude of  $\sigma_K$ . The validity of this assumption is difficult to prove because many of the covariances involved are impossible to determine; however, sample calculations suggest that this simplification leads to *minimum* estimates of  $\sigma_K$ . With this qualification in mind, we used the Monte Carlo method of uncertainty propagation to estimate  $\sigma_K$ . This involved:

- (1) Assignment of  $1\sigma$  errors to the various parameters used in calculating  $K$ ;
- (2) Generation of a 200 element array for each input parameters, which consists of a population of values normally distributed about the "accepted value";
- (3) Calculation of  $K$  using a randomly chosen element from each parameter's array; and
- (4) A total of 100 iterations of the previous step, leading to a normally distributed population of  $K$  from which a standard deviation is calculated.

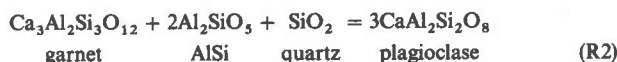
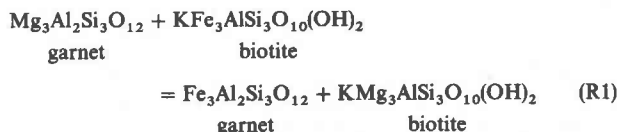
Once  $\sigma_K$  is estimated by this method, then the uncertainty in  $[y]$  may be calculated using the basic error propagation equation. For  $Z = f(q, r, \dots)$ :

$$\sigma_z^2 = (\partial Z/\partial q)^2 \sigma_q^2 + (\partial Z/\partial r)^2 \sigma_r^2 + 2\rho_{qr} \sigma_q \sigma_r (\partial Z/\partial q)(\partial Z/\partial r) + \dots \quad (3)$$

where  $q, r, \dots$  are the various input parameters;  $\sigma_q, \sigma_r, \dots$  are their uncertainties, and terms such as  $\rho_{qr}$  are correlation coefficients which describe dependence between uncertainties in the various parameters. We will refer subsequently to the combined Monte Carlo-partial differential method of estimating uncertainties in  $[y]$  as "MCPD".

### Application—pelitic schists

Pelitic schists and gneisses have proven to be reliable qualitative indicators of metamorphic grade over a wide range of  $P$ - $T$  conditions (e.g., Thompson, 1976b). A variety of quantitative geologic thermobarometers have been proposed for pelitic systems, and two of the best calibrated are



Although a variety of empirical and experimental calibrations exist for these equilibria, we feel that the most reliable are those of Ferry and Spear (1978) for (R1) and of Newton and Haselton (1981) for (R2). Several studies (e.g., Hodges and Spear, 1982) have shown that these calibrations consistently yield  $P$ - $T$  estimates which are geologically reasonable for samples which were not substantially retrograded during uplift and cooling.

Using (R1) and (R2) to estimate  $P$  and  $T$ , we explored the possibility of other useful thermobarometers for pelitic assemblages. We considered the assemblage garnet (gar)-biotite (bio)-muscovite (mu)-plagioclase (pl)-aluminum silicate (AlSi)-quartz (q) in the model system  $\text{K}_2\text{O}-\text{CaO}-\text{FeO}-\text{Al}_2\text{O}_3-\text{SiO}_2-\text{H}_2\text{O}$ . Table 1 shows our choice of phase components for this assemblage.

Table 2 shows the reactions examined in this study. Of these, only two are linearly independent; however, all were calibrated using the technique described above and the resulting thermodynamic constants were compared to those obtainable through linear combinations. Calibrations of the equilibria in Table 2 were based on published compositional data for 59 pelitic samples (Table 3). In choosing this data set, we were attentive to: 1) assemblages which contained all of the necessary phases; 2) the probability of chemical equilibrium between the phases involved; 3) the lack of evidence for significant retrogression; and 4) the completeness of published analyses (especially Fe in muscovite). The last of these requirements was particularly difficult to achieve. Despite our efforts, only 28 of the 59 samples could be used to calibrate the reactions involving Tschermak exchange in muscovite ( $\text{Al}_2\text{Fe}_{-1}\text{Si}_{-1}$ ) because of insufficient published analytical data. In some cases, both rim and core compositions were reported for garnet and/or biotite; we used rim compositions for calibration purposes. Fletcher and Greenwood (1979) reported a range

Table 1. Model phase components

Phase	Components
Garnet	Fe <sub>3</sub> Al <sub>2</sub> Si <sub>3</sub> O <sub>12</sub> (almandine) Ca <sub>3</sub> Al <sub>2</sub> Si <sub>3</sub> O <sub>12</sub> (grossular)
Biotite	KFe <sub>3</sub> AlSi <sub>3</sub> O <sub>10</sub> (OH) <sub>2</sub> (annite)
Muscovite	KAl <sub>3</sub> Si <sub>3</sub> O <sub>10</sub> (OH) <sub>2</sub> (muscovite) Al <sub>2</sub> Fe <sub>-1</sub> Si <sub>-1</sub> (Tschermak exchange)
Plagioclase	CaAl <sub>2</sub> Si <sub>2</sub> O <sub>8</sub> (anorthite)
Aluminum Silicate	Al <sub>2</sub> SiO <sub>5</sub> (AlSi)
Quartz	SiO <sub>2</sub> (quartz)

of plagioclase compositions; we used their highest Ca analyses with the justification that prograde plagioclase zonation usually is characterized by increasing anorthite component from core to rim (e.g., Ghent, 1976). For samples containing more than one aluminum silicate, we treated kyanite + sillimanite assemblages as if they contained kyanite alone and andalusite + sillimanite assemblages as if sillimanite was the only AlSi phase. Sample calculations using the alternative treatments did not result in significantly different calibrations.

Activity-composition relationships used to calculate equilibrium constants for (R1)–(R12) in natural samples are shown in Table 4. The derivation of most of these formulations is discussed in Hodges and Spear (1982) and Hodges and Royden (1984). The  $a_{is}$  model in Table 4 implies one-site mixing and full octahedral site occupancy. Although this simple model seems to work quite well in the calculations presented below, we suggest that the applica-

bility of this formulation to a given sample be carefully examined before use.

Molar volume data were taken from Helgeson et al. (1978) with a few exceptions. Robie et al. (1978) supplied the molar volume of pyrope (113.3 cm<sup>3</sup>). The molar volume of grossular was calculated using the expression proposed by Newton and Haselton (1981), which we modified slightly by substituting  $(1 - X_{gr})$  for  $X_{al}$  or  $X_{py}$  in order to partially account for the effects of Mn on grossular mixing. Finally, we estimated the molar volume of Tschermak exchange in dioctahedral micas as follows. We can define

$$Al_2Si_{-1}Fe_{-1} = KAl_3Si_3O_{10}(OH)_2 - KFeAlSi_4O_{10}(OH)_2 \quad (7)$$

Tschermak                      muscovite                      Fe celadonite

Unfortunately, although molar volume data exist for Mg celadonite, they do not exist for Fe celadonite. We circumvent this problem by assuming that  $\Delta V$  is the same for FeMg<sub>-1</sub> in both dioctahedral and trioctahedral micas. Thus,  $\Delta V_{is} = V_{muscovite} - [V_{Mg\ celadonite} + 1/3 (V_{annite} - V_{phlogopite})] = -17.9 \text{ cm}^3$ .

Pressures and temperatures were calculated for all samples through simultaneous solution of equilibrium constant equations for (R1) using the Ferry and Spear (1978) calibration, and (R2), using the Newton and Haselton (1981) calibration (Table 6). The results of these calculations are shown in Table 3. The values are geologically reasonable and agree well with the expected aluminum silicate stability fields, given the phase boundaries of Holdaway (1971) and their respective uncertainties. This suggests that (R1) and (R2), used with the solution models in Table 4, yield fundamentally correct  $P$ - $T$  estimates over the compositional ranges encountered in the sample set. Since the empirical calibrations presented below are strongly dependent on the chosen solution models, it is important to remember that

Table 2. Net-transfer reactions

(R3)	Fe <sub>3</sub> Al <sub>2</sub> Si <sub>3</sub> O <sub>12</sub> + Ca <sub>3</sub> Al <sub>2</sub> Si <sub>3</sub> O <sub>12</sub> + KAl <sub>3</sub> Si <sub>3</sub> O <sub>10</sub> (OH) <sub>2</sub> = 3 CaAl <sub>2</sub> Si <sub>2</sub> O <sub>8</sub> + KFe <sub>3</sub> AlSi <sub>3</sub> O <sub>10</sub> (OH) <sub>2</sub>
	gar                      gar                      mu                      pl                      bio
(R4)	Fe <sub>3</sub> Al <sub>2</sub> Si <sub>3</sub> O <sub>12</sub> + 2 Ca <sub>3</sub> Al <sub>2</sub> Si <sub>3</sub> O <sub>12</sub> + 3 Al <sub>2</sub> Si <sub>-1</sub> Fe <sub>-1</sub> + 6 SiO <sub>2</sub> = 6 CaAl <sub>2</sub> Si <sub>2</sub> O <sub>8</sub>
	gar                      gar                      mu                      q                      pl
(R5)	KFe <sub>3</sub> AlSi <sub>3</sub> O <sub>10</sub> (OH) <sub>2</sub> + Ca <sub>3</sub> Al <sub>2</sub> Si <sub>3</sub> O <sub>12</sub> + 3 Al <sub>2</sub> Si <sub>-1</sub> Fe <sub>-1</sub> + 6 SiO <sub>2</sub> = 3 CaAl <sub>2</sub> Si <sub>2</sub> O <sub>8</sub> + KAl <sub>3</sub> Si <sub>3</sub> O <sub>10</sub> (OH) <sub>2</sub>
	bio                      gar                      mu                      q                      pl                      mu
(R6)	2 KFe <sub>3</sub> AlSi <sub>3</sub> O <sub>10</sub> (OH) <sub>2</sub> + 3 Al <sub>2</sub> Si <sub>-1</sub> Fe <sub>-1</sub> + 6 SiO <sub>2</sub> = 2 KAl <sub>3</sub> Si <sub>3</sub> O <sub>10</sub> (OH) <sub>2</sub> + Fe <sub>3</sub> Al <sub>2</sub> Si <sub>3</sub> O <sub>12</sub>
	bio                      mu                      q                      mu                      gar
(R7)	Fe <sub>3</sub> Al <sub>2</sub> Si <sub>3</sub> O <sub>12</sub> + 3 Al <sub>2</sub> Si <sub>-1</sub> Fe <sub>-1</sub> + 4 SiO <sub>2</sub> = 4 Al <sub>2</sub> SiO <sub>5</sub>
	gar                      mu                      q                      AlSi
(R8)	12 CaAl <sub>2</sub> Si <sub>2</sub> O <sub>8</sub> + Fe <sub>3</sub> Al <sub>2</sub> Si <sub>3</sub> O <sub>12</sub> + 3 Al <sub>2</sub> Si <sub>-1</sub> Fe <sub>-1</sub> = 12 Al <sub>2</sub> SiO <sub>5</sub> + 4 Ca <sub>3</sub> Al <sub>2</sub> Si <sub>3</sub> O <sub>12</sub>
	pl                      gar                      mu                      AlSi                      gar
(R9)	4 KAl <sub>3</sub> Si <sub>3</sub> O <sub>10</sub> (OH) <sub>2</sub> + 5 Fe <sub>3</sub> Al <sub>2</sub> Si <sub>3</sub> O <sub>12</sub> + 3 Al <sub>2</sub> Si <sub>-1</sub> Fe <sub>-1</sub> = 12 Al <sub>2</sub> SiO <sub>5</sub> + 4 KFe <sub>3</sub> AlSi <sub>3</sub> O <sub>10</sub> (OH) <sub>2</sub>
	mu                      gar                      mu                      AlSi                      bio
(R10)	KFe <sub>3</sub> AlSi <sub>3</sub> O <sub>10</sub> (OH) <sub>2</sub> + 3 Al <sub>2</sub> Si <sub>-1</sub> Fe <sub>-1</sub> + 5 SiO <sub>2</sub> = 2 Al <sub>2</sub> SiO <sub>5</sub> + KAl <sub>3</sub> Si <sub>3</sub> O <sub>10</sub> (OH) <sub>2</sub>
	bio                      mu                      q                      AlSi                      mu
(R11)	15 CaAl <sub>2</sub> Si <sub>2</sub> O <sub>8</sub> + KFe <sub>3</sub> AlSi <sub>3</sub> O <sub>10</sub> (OH) <sub>2</sub> + 3 Al <sub>2</sub> Si <sub>-1</sub> Fe <sub>-1</sub> = 12 Al <sub>2</sub> SiO <sub>5</sub> + KAl <sub>3</sub> Si <sub>3</sub> O <sub>10</sub> (OH) <sub>2</sub> + 5 Ca <sub>3</sub> Al <sub>2</sub> Si <sub>3</sub> O <sub>12</sub>
	pl                      bio                      mu                      AlSi                      mu                      gar
(R12)	KAl <sub>3</sub> Si <sub>3</sub> O <sub>10</sub> (OH) <sub>2</sub> + Fe <sub>3</sub> Al <sub>2</sub> Si <sub>3</sub> O <sub>12</sub> = KFe <sub>3</sub> AlSi <sub>3</sub> O <sub>10</sub> (OH) <sub>2</sub> + 2 Al <sub>2</sub> SiO <sub>5</sub> + SiO <sub>2</sub>
	mu                      gar                      bio                      AlSi                      q

Table 3. Sample set

Reference	Sample	AlSi Phase	T(°C)	P(bars)
Hodges and Spear(1982)	79-788	Si1	476	3399
	79-800	Si1	518	3978
	79-90A	Si1	498	3713
	79-92D	Si1	499	3284
	79-145E	Si1	502	2460
	79-146B	Si1	537	3520
	79-1460	Si1	478	2595
Ferry (1980)	56A	And	527	3259
	246A	And	517	3306
	388A	Si1	572	3289
	663A	Si1	600	4220
	666A	Si1	542	3469
	674A	Si1	568	3145
	675-4	Si1	568	3101
	675-5	Si1	600	4032
	905A	Si1	560	4152
	917A	And	528	3430
	928A	And	559	3891
	953A	And	493	3149
	969B	Si1	571	2700
	980A	And	494	2937
	1001A	And	534	3434
	1006A	And	505	2968
	1010A	And	547	2889
	1104-1	Si1	546	4075
	Tracy (1978)	892U	Si1	583
869		Si1	553	3788
871		Si1	605	3916
C26A		Si1	561	2612
595C		Si1	757	7032
M34		Si1	527	4385
Pigage (1982)	373	Ky	575	6167
	121	Ky	561	5181
	367	Ky	573	6335
	82	Ky	550	5311
	398	Si1	555	4544
	492	Ky	556	4859
	223	Ky	554	5052
	2-376	Ky	588	6476
	2-13	Si1	552	5354
	74	Si1	610	6546
59	Si1	582	5843	
40	Si1	557	4672	
Pigage (1976)	2	Ky	563	7451
	3	Ky	586	6783
	4	Ky	569	8204
	5	Ky	586	5850
	6	Ky	614	6708
7	Si1	615	6138	
Fletcher and Greenwood (1970)	5	Ky	672	8116
	6	Ky	551	5843
	7	Ky	658	4856
	8	Ky	601	6992
	9	Ky	529	4632
	11	Ky	573	6972
	12	Ky	612	5730
	13	Ky	743	9562
	14	Ky	663	7326
	15	Si1	647	6162

application of these thermobarometers to samples with mineral chemistry significantly different from that encountered in the sample set should proceed with caution. Specifically, we advise against the use of these calibrations for samples in which garnet has >25 mole% spessartine and biotite has >20 mole% Al or >5 mole% Ti in the octahedral site.

### Uncertainty estimation

Assignment of uncertainties to the various parameters used to calculate [x] and [y] was made difficult by interlaboratory variations in microprobe techniques and by the fact that some of the uncertainties are simply unknown. We assigned a blanket 1 $\sigma$  uncertainty of 3% mole fraction of the published microprobe data used to calculate K for the reactions in Table 2. Uncertainties in activity models shown in Table 4 could be quite large but are impossible to quantify; consequently, we assumed no uncertainty in these

relationships. Uncertainties in molar volume data are often poorly known, and their propagation through  $\Delta V$  calculations is compounded by our ignorance of many of the coefficients of isothermal compressibility and thermal expansion necessary to convert tabulated data to the pressure and temperature of interest. In this exercise, we assumed  $\sigma_{\Delta V} = 0$ .

Some of the most significant sources of uncertainty in [y] and [x] stem from uncertainties in P and T calculated from (R1)–(R2). Many different estimates of these uncertainties have appeared in the literature, and most are probably optimistic. For regression purposes, we adopted values of  $\sigma_T = 50^\circ\text{C}$  and  $\sigma_P = 1000$  bars, reflecting a general consensus in the literature based on the reproducibility of (R1)–(R2) P and T for several samples from single geographic locations (e.g., Ferry, 1980; Ghent et al., 1982; Hodges and Spear, 1982).

Significant positive correlation is likely between  $\sigma_P$  and  $\sigma_T$  (Steltenpohl and Bartley, 1984); for simplicity in calculation, we assigned  $\rho_{PT} = 1.0$  in equation (2). It is virtually impossible to quantify  $\rho_{PK}$  and  $\rho_{TK}$ ; we assumed a value of 1.0 for each coefficient. The effect of these assumptions is to

Table 4. Activity–composition relationships

$$a_{al} = [X_{al} \cdot \exp(((1.5T(^{\circ}\text{K}) - 3300) \cdot (X_{py} X_{gr})) / RT(^{\circ}\text{K})))]^3$$

$$a_{py} = [X_{py} \cdot \exp(((3300 - 1.5T(^{\circ}\text{K})) \cdot (X_{gr}^2 + X_{al} X_{gr} + X_{gr} X_{sp})) / RT(^{\circ}\text{K})))]^3$$

$$a_{gr} = [X_{gr} \cdot \exp(((3300 - 1.5T(^{\circ}\text{K})) \cdot (X_{py}^2 + X_{al} X_{py} + X_{py} X_{sp})) / RT(^{\circ}\text{K})))]^3$$

$$a_{an} = X_{an} \cdot \exp(610.34/T(^{\circ}\text{K}) - .3837)$$

$$a_{mu} = (X_{kmu} X_{al\mu}^2) \cdot \exp(((X_{namu} X_{al\mu}^2)^2 \cdot (W_{mu} + 2X_{kmu} X_{al\mu}^2 (W_{pa} - W_{mu}))) / RT(^{\circ}\text{K}))$$

$$a_{ann} = (X_{ann})^3$$

$$a_{ph} = (X_{ph})^3$$

$$a_{ts} = (2X_{al\mu} - 1) / 2X_{femu}$$

$$X_{al} = \text{Fe/Fe+Mg+Ca+Mn in garnet}$$

$$X_{py} = \text{Mg/Fe+Mg+Ca+Mn in garnet}$$

$$X_{gr} = \text{Ca/Fe+Mg+Ca+Mn in garnet}$$

$$X_{sp} = \text{Mn/Fe+Mg+Ca+Mn in garnet}$$

$$X_{an} = \text{Ca/Ca+Na+K in plagioclase}$$

$$X_{ab} = \text{Na/Ca+Na+K in plagioclase}$$

$$X_{femu} = \text{Fe/Fe+Mg+Mn+Ti+AlVI in muscovite}$$

$$X_{kmu} = \text{K/Ca+Na+K in muscovite}$$

$$X_{namu} = \text{Na/Ca+Na+K in muscovite}$$

$$X_{al\mu} = \text{AlVI/Fe+Mg+Mn+Ti+AlVI in muscovite}$$

$$X_{ann} = \text{Fe/Fe+Mg+Ti+AlVI in biotite}$$

$$X_{ph} = \text{Mg/Fe+Mg+Ti+AlVI in biotite}$$

$$W_{pa} = 2923.1 + 0.1590 P(\text{bars}) + 0.1698T(^{\circ}\text{K})$$

$$W_{mu} = 4650.1 + 0.1090 P(\text{bars}) + 0.3954T(^{\circ}\text{K})$$

maximize the effect of covariance terms in (2) and thus increase the uncertainty estimates for the empirical calibrations. Despite this, the fact that we have ignored potentially large but unconstrained uncertainties in activity models,  $\Delta V$ , etc. suggests that the calibration uncertainties presented below are *minimum* estimates.

### Results

Using mineral composition data for the samples in Table 3, the activity models in Table 4, and error estimates from the previous section, we used the MCPD method to establish errors in  $[x]$  and  $[y]$  for (R3) through (R12). Because both variables are functions of  $T$ ,  $\sigma_{[x]}$  and  $\sigma_{[y]}$  will be correlated in most instances. The York (1969) regression method accounts for this correlation through a blanket correlation coefficient for all  $\sigma_{[x]}$  and  $\sigma_{[y]}$  for a given data set. For each reaction, we calculated this coefficient using simple, least-squares linear regression of  $\sigma_{[x]}$  vs.  $\sigma_{[y]}$  and the standard correlation coefficient equation. Calculated values ranged from about  $-0.1$  to  $+0.9$ . Table 5 shows the thermodynamic constants and their uncertainties (reported at the  $1\sigma$  confidence level) as derived through regression analysis. The quality of the regressions varies from excellent (e.g., (R3)—Fig. 1a) to poor (e.g. (R9-K)—Fig. 1b); however, some general observations can be made.

First, the quality of (R3), (R4), and (R11) regression statistics support the argument that the activity models in Table 4 and the  $P$ - $T$  conditions calculated from (R1) and (R2) are fundamentally correct. Second, regression statistics for sillimanite-bearing samples are generally much better than those for kyanite-bearing samples. This may be due to the fact that fewer samples were used to calibrate kyanite-dependent reactions, and that the Fletcher and Greenwood (1979) and Pigage (1982) samples show textural evidence suggesting long and complicated metamorphic histories. Thus, it is possible that not all of the phase compositions in these samples represent chemical equilibrium. Because of the overwhelmingly better quality of the sillimanite-dependent calibrations, we used linear combinations of the sillimanite dependent reactions with kyanite = sillimanite (Holdaway, 1971) to arrive at better estimates of  $\Delta H$  and

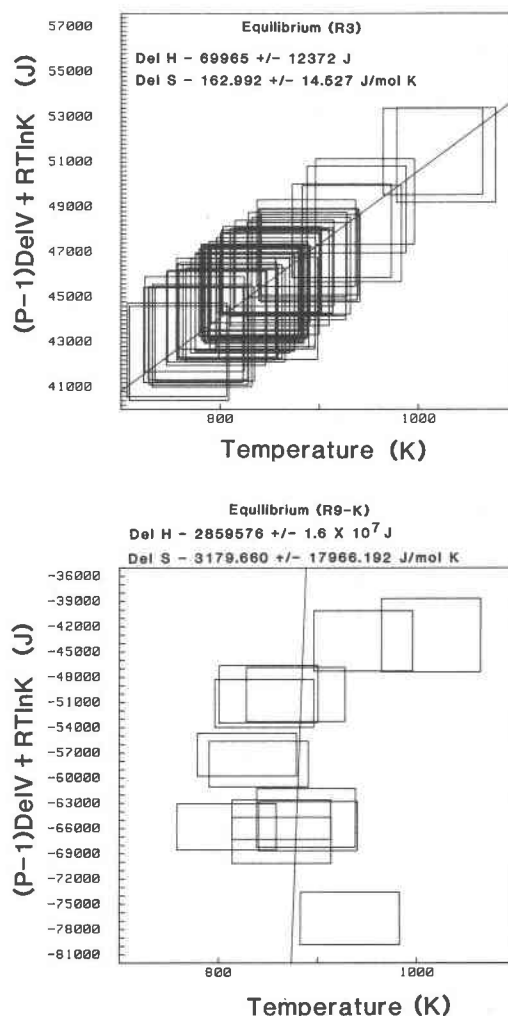


Fig. 1. Sample regression plots: a. (R3); b. (R9-K). Units for  $\Delta H$  and  $\Delta S$  are J and J/mol $^{\circ}$ K, respectively. Error boxes indicate  $1\sigma$  uncertainties.

Table 5. Regression results

Reaction	$\Delta H$ (J)	$\Delta S$ (J/mol $^{\circ}$ K)
(R3)	69965 +/- 12372	162.992 +/- 14.527
(R4)	189029 +/- 31096	352.644 +/- 35.719
(R5)	127813 +/- 21401	199.535 +/- 24.656
(R6)	173891 +/- 56384	171.205 +/- 65.442
(R7-S)	140432 +/- 13694	131.332 +/- 16.075
(R7-K)	-3836820 +/- $5.6 \times 10^7$	-4396.313 +/- 63216.859
(R8-S)	-51359 +/- 38275	-413.488 +/- 44.484
(R8-K)	-183895 +/- 110257	-610.948 +/- 125.323
(R9-S)	242827 +/- 61781	252.115 +/- 73.341
(R9-K)	2859576 +/- $1.6 \times 10^7$	3179.660 +/- 17966.192
(R10-S)	102897 +/- 11874	87.241 +/- 13.924
(R10-K)	-426145 +/- 934965	-517.067 +/- 1061.456
(R11-S)	-124432 +/- 38966	-579.128 +/- 43.886
(R11-K)	-256073 +/- 136223	-776.764 +/- 154.716
(R12-S)	41894 +/- 12314	49.120 +/- 14.581
(R12-K)	-501741 +/- $1.5 \times 10^6$	-585.040 +/- 5002.738

$\Delta S$  for kyanite-dependent (R7)–(R12). Together with the AlSi-independent and sillimanite-dependent calibrations from Table 5, these constitute our “preferred” calibrations shown in Table 6.

Finally, we observe that the calibration quality for plagioclase-dependent reactions is consistently better than that for plagioclase-independent reactions. This is perhaps not surprising, since all of the reactions involving plagioclase owe their fairly large  $\Delta V$  to the same anorthite-grossular density change that characterizes (R2) and forms the pressure basis for the calibration procedure. In other words, it seems likely that reactions which are chemically similar to the experimentally based thermobarometers used for calibration will yield better calibration statistics than those which are not similar.

Table 6. Preferred calibrations

Reaction	$\Delta H$ (J)	$\Delta S$ (J/mol $^{\circ}K$ )
(R1)*	52108	19,506
(R2-A)**	34401	119,616
(R2-S)**	40819	127,399
(R2-K)**	55865	153,591
(R3)	69965 +/- 12372	162,992 +/- 14,527
(R4)	189029 +/- 31096	352,644 +/- 35,719
(R5)	127813 +/- 21401	199,535 +/- 24,656
(R6)	173891 +/- 56384	171,205 +/- 65,442
(R7-S)	140432 +/- 13694	131,332 +/- 16,075
(R7-K)	110340 +/- 13720	78,948 +/- 16,245
(R8-S)	-51359 +/- 38275	-413,488 +/- 44,484
(R8-K)	-141635 +/- 38357	-570,640 +/- 45,036
(R9-S)	242827 +/- 61781	252,115 +/- 73,341
(R9-K)	152951 +/- 61832	94,963 +/- 73,677
(R10-S)	102897 +/- 11874	87,241 +/- 13,924
(R10-K)	87851 +/- 11881	61,049 +/- 13,973
(R11-S)	-124432 +/- 38966	-579,128 +/- 43,886
(R11-K)	-214708 +/- 39047	-736,280 +/- 44,446
(R12-S)	41894 +/- 12314	49,120 +/- 14,581
(R12-K)	26848 +/- 12321	22,928 +/- 14,628

\* - Ferry and Spear (1978)

\*\* - Newton and Haselton (1981)

### Comparison with other calibrations

Of the ten new thermobarometers considered here, only (R3) and (R12) have been calibrated previously. Ghent and Stout (1981) calculated  $\Delta H$  and  $\Delta S$  for (R3) using a variety of techniques, including simple, least-squares linear regression analysis of natural samples. The empirical approach yielded the most geologically reasonable  $P$ - $T$  estimates for an independent set of natural samples.

The thermodynamic constants empirically derived by Ghent and Stout (1981) are quite different from those which we obtained ( $\Delta H = 17257$  J vs. 69965 J;  $\Delta S = 92.303$  J/mol $^{\circ}K$  vs. 162.992 J/mol $^{\circ}K$ ). This discrepancy may reflect: (1) differences in regression technique; (2) differences in assumed activity models; (3) differences in the calibration used for obtaining  $P$  and  $T$  estimates; and/or 4) differences in the number of samples ( $n$ ) used and the overall  $P$ - $T$  range represented (Ghent and Stout:  $n = 19$ ,  $P = 3500$ -6000 bar,  $T = 450$ -600 $^{\circ}C$ ; this study:  $n = 59$ ,  $P = 2500$ -9500 bar,  $T = 480$ -750 $^{\circ}C$ ).

Thompson (1976a) and Tracy et al. (1976) suggested calibrations of (R12-S) based on tabulated entropy and volume data for the participating phases, as well as additional constraints from experimental data for other reactions. In both papers,  $dP/dT$  for the end-member (R12-S) reaction was estimated as  $\sim 8$  bar/ $^{\circ}C$ . Fletcher and Greenwood (1979) used calibrations of (R12-S) and (R12-K) based on tabulated thermochemical data in order to estimate metamorphic conditions in the Penfold Creek area of British Columbia. Although Fletcher and Greenwood used complete heat capacity equations to extrapolate the thermochemical data, calculation of the Clapyron slope for end-member (R12-S) and (R12-K) using their preferred  $\Delta S^{\circ}$  and  $\Delta H^{\circ}$  (1 bar, 298 $^{\circ}K$ ) and assuming  $\Delta C_p = 0$  yields 35 bar/ $^{\circ}C$  and 50 bar/ $^{\circ}C$ , respectively. Our preferred calibrations (Table 6) yield 24 bar/ $^{\circ}C$  for (R12-S) and 25 bar/ $^{\circ}C$  for (R12-K).

We tested the relative quality of the various calibrations of (R3) and (R12) by simultaneously solving each with (R1) to obtain  $P$ - $T$  estimates for seven kyanite-bearing pelitic samples from the Eford area, northern Norway (Hodges and Royden, 1984). These  $P$ - $T$  estimates were then compared with (R1)-(R2) pressures and temperatures, and mean deviations in  $P$  and  $T$  ( $\Delta P_m$ ,  $\Delta T_m$ ) were calculated. The (R3) calibration of Ghent and Stout (1981) yielded  $\Delta P_m = -1059$  bar and  $\Delta T_m = -1.6^{\circ}C$ , while our calibration gave a significantly better fit of  $\Delta P_m = 47$  bar and  $\Delta T_m = 0.6^{\circ}C$ . None of the (R12-K) calibrations reproduced the (R1)-(R2)  $P$ - $T$  estimates particularly well: (1) Tracy et al. (1976) -  $\Delta P_m = 4967$  bar,  $\Delta T_m = 16^{\circ}C$ ; (2) Fletcher and Greenwood (1979) -  $\Delta P_m = -4092$  b;  $\Delta T_m = -9.9^{\circ}C$ ; and (3) this study -  $\Delta P_m = -3348$  b;  $\Delta T_m = -14^{\circ}C$ . These results suggest that our calibration for (R12), while providing the best match to (R1)-(R2)  $P$ - $T$  estimates, is useful only for estimating minimum pressures and temperatures of crystallization.

### Discussion

A modification of the MCPD method may be used to propagate uncertainties in  $\Delta H$  and  $\Delta S$  (Table 6) as well as uncertainties in microprobe data, into uncertainties in  $P$ - $T$  estimates based on a particular reaction. Table 7 shows  $\sigma_T$  at constant  $P$  and  $\sigma_P$  at constant  $T$  for a sillimanite-bearing sample (79-78B; Hodges and Spear, 1982) and a kyanite-bearing sample (2; Pigage, 1976). These uncertainties are extremely large:  $\sigma_T$  ranges from 95 to 930  $^{\circ}C$ ,  $\sigma_P$  from 2044 to 97699 bars. All of the equilibria are better indicators of  $T$  than  $P$  as a consequence of their moderately high  $dP/dT$  for compositional ranges commonly encountered in natural assemblages. Equilibria (R3), (R11), and (R4) provide  $P$ - $T$  estimates with the highest precision, principally due to superior regression statistics. Given that the regression analysis was based on the optimistic assumption of  $\sigma_T = 50^{\circ}C$  and  $\sigma_P = 1000$  bar for (R1)-(R2)  $P$ - $T$  estimates, the values in Table 7 are assumed to be minimum estimates of precision. In general, our calculations suggest that even the "best" empirical calibrations are two to five times more imprecise than the experimental calibrations on which they are based.

It is important to remember that much of the uncertainty in  $P$ - $T$  estimates stems from uncertainties in  $\Delta H$  and  $\Delta S$ , while uncertainties in microprobe data represent a relatively small part of the cumulative uncertainty. Assumptions of  $\sigma_{\Delta H} = 0$  and  $\sigma_{\Delta S} = 0$  result in 60-75% reductions in  $\sigma_T$  and  $\sigma_P$  for (R3)-(R12). This implies that estimating differences in  $P$ - $T$  between samples, which is the goal of most tectonic applications of thermobarometry, can be done more precisely than estimating absolute  $P$ - $T$  for individual samples.

### Conclusions

We have presented a method of propagating the uncertainties involved in empirical calibration into uncertainties in the  $P$ - $T$  estimates obtained using empirical thermobarometry.

Table 7. Pressure-temperature precision

Reaction	79-78B (Hodges and Spear, 1982)		2 (Pigage, 1976)	
	$\sigma_T$ ( $^{\circ}\text{C}$ at $P = 3399$ bars)	$\sigma_P$ (bars at $T = 476$ $^{\circ}\text{C}$ )	$\sigma_T$ ( $^{\circ}\text{C}$ at $P = 7451$ bars)	$\sigma_P$ (bars at $T = 563^{\circ}\text{C}$ )
(R3)	131	2168	140	2664
(R4)	127	2521	128	2996
(R5)	137	3248	132	3785
(R6)	357	95007	333	97699
(R7)	95	3765	147	7828
(R8)	355	4025	149	2674
(R9)	246	5793	771	13982
(R10)	112	5657	134	9843
(R11)	185	2360	112	2044
(R12)	309	7178	930	18376

meters. This technique yields only minimum estimates of precision because some of the propagated uncertainties are imprecisely known and several potentially important covariance terms are uncertain. Nevertheless, the method provides important information concerning the relative precision of empirical thermobarometers, and indicates that experimental calibrations are much more precise than their empirical counterparts.

We have derived new empirical calibrations for ten thermobarometers appropriate for pelitic assemblages (Table 6). The values of  $\sigma_P$  and  $\sigma_T$  in Table 7 suggest that the relative quality of these calibrations is (R3) > (R11) > (R4) > (R5) > (R7) > (R8) > (R10) > (R9) > (R12) > (R6). Equilibria (R3), (R4) and (R5) will be especially useful for the common AlSi-free assemblage: garnet-biotite-muscovite-plagioclase-quartz. Equilibrium (R4) could serve as a pressure indicator for biotite-free assemblages provided that some independent means of temperature estimation were available.

If the thermodynamic properties of the Tschermak exchange are similar for dioctahedral micas and amphiboles, then (R4) and (R11) may be useful thermobarometers for mafic schists. Either of these equilibria could be solved simultaneously with the garnet-hornblende Fe-Mg geothermometer (Graham and Powell, 1984) to obtain P-T estimates for garnet + clinopyroxene + biotite + plagioclase  $\pm$  quartz  $\pm$  aluminum silicate assemblages.

### Acknowledgments

We would like to thank Kevin Furlong for introducing us to the perils of statistical rigor. Howard Day, Jack Rice, Leigh Royden, Jane Selverstone, Frank Spear, and Doug Walker contributed to this paper through either lengthy discussion or careful critical review. This research was partially funded through a National Science Foundation Grant (EAR-8407730) awarded to KVH.

### References

- Anderson, G. M. (1976) Error propagation by the Monte Carlo method in geochemical calculations. *Geochimica et Cosmochimica Acta*, 40, 1533-1538.
- Anderson, G. M. (1977) Uncertainties in calculations involving thermodynamic data. In H. J. Greenwood, Ed., *Short Course in Application of Thermodynamics to Petrology and Ore Deposits*, p. 199-215, Mineralogical Association of Canada.
- Brooks, C., Hart, S. R., and Wendt, I. (1972) Realistic use of two-error regression treatments as applied to Rubidium-Strontium data. *Reviews of Geophysics and Space Physics*, 10, 551-557.
- Ferry, J. M. (1980) A comparative study of geothermometers and geobarometers in pelitic schists from southern-central Maine. *American Mineralogist*, 65, 720-732.
- Ferry, J. M. and Spear, F. S. (1978) Experimental calibration of the partitioning of Fe and Mg between biotite and garnet. *Contributions to Mineralogy and Petrology*, 66, 113-117.
- Fletcher, C. J. N. and Greenwood, H. J. (1979) Metamorphism and structure of Penfold Creek area, near Quesnel Lake, British Columbia. *Journal of Petrology*, 20, 743-794.
- Ghent, E. D. (1976) Plagioclase-garnet- $\text{Al}_2\text{SiO}_5$ -quartz: a potential geobarometer-geothermometer. *American Mineralogist*, 61, 710-714.
- Ghent, E. D. and Stout, M. Z. (1981) Geobarometry and geothermometry of plagioclase-biotite-garnet-muscovite assemblages. *Contributions to Mineralogy and Petrology*, 76, 92-97.
- Ghent, E. D., Knitter, C. C., Raeside, R. P., and Stout, M. Z. (1982) Geothermometry and geobarometry of pelitic rocks, upper kyanite and sillimanite zones, Mica Creek area, British Columbia. *Canadian Mineralogist*, 20, 295-305.
- Graham, C. M. and Powell, R. (1984) A garnet-hornblende geothermometer: calibration, testing, and application to the Pelona Schist, Southern California. *Journal of Metamorphic Geology*, 2, 13-31.
- Helgeson, H. C., Delany, J. M., Nesbitt, H. W. and Bird, D. K. (1978) Summary and critique of the thermodynamic properties of rock forming minerals. *American Journal of Science*, 278-A.
- Hodges, K. V. and Spear, F. S. (1982) Geothermometry, geobarometry and the  $\text{Al}_2\text{SiO}_5$  triple point at Mt. Moosilauke, New Hampshire. *American Mineralogist*, 67, 1118-1134.
- Hodges, K. V. and Royden, L. (1984) Geologic thermobarometry of retrograded metamorphic rocks: an indication of the uplift trajectory of a portion of the northern Scandinavian Caledonides. *Journal of Geophysical Research*, 89, 7077-7090.
- Holdaway, M. J. (1971) Stability of andalusite and the aluminosilicate phase diagram. *American Journal of Science*, 271, 97-131.
- Newton, R. C. and Haselton, H. T. (1981) Thermodynamics of the garnet-plagioclase- $\text{Al}_2\text{SiO}_5$ -quartz geobarometer. In R. C. Newton et al., Eds., *Thermodynamics of Minerals and Melts*, p. 131-147. Springer-Verlag, New York.
- Pigage, L. C. (1976) Metamorphism of the Settler Schist, south-

- west of Yale, British Columbia. *Canadian Journal of Earth Sciences*, 13, 405-421.
- Pigage, L. C. (1982) Linear regression analysis of sillimanite-forming reactions at Azure Lake, British Columbia. *Canadian Mineralogist*, 20, 349-378.
- Robie, R. A., Hemingway, B. S., and Fisher, J. R. (1978) Thermodynamic properties of minerals and related substances at 298.13K and 1 bar ( $10^5$  Pascals) pressure and at higher temperatures. *U.S. Geological Survey Bulletin*, 1452, 456 pp.
- Steltenpohl, M. and Bartley, J. M. (1984) Statistical evaluation of P-T trajectories based on elemental partitioning geothermometers and geobarometers. *Geological Society of America Abstracts with Programs*, 16, 667.
- Thompson, A. B. (1976a) Mineral reactions in pelitic rocks: II. Calculation of some P-T-X(Fe-Mg) phase relations. *American Journal of Science*, 276, 425-454.
- Thompson, A. B. (1976b) Mineral reactions in pelitic rocks: I. Prediction of P-T-X(Fe-Mg) phase relations. *American Journal of Science*, 276, 401-424.
- Tracy, R. J. (1978) High grade metamorphic reactions and partial melting in pelitic schist, west central Massachusetts. *American Journal of Science*, 278, 150-178.
- Tracy, R. J., Robinson, P., and Thompson, A. B. (1976) Garnet composition and zoning in the determination of temperature and pressure of metamorphism, central Massachusetts. *American Mineralogist*, 61, 762-775.
- York, D. (1969) Least squares fitting of a straight line with correlated errors. *Earth and Planetary Science Letters*, 5, 320-324.

*Manuscript received, August 6, 1984;  
accepted for publication, March 14, 1985.*